Jan Braun, BSc

Impact of active site mutations in *E.coli* nitrile reductase QueF on substrate affinity, activity and side reactions

MASTER'S THESIS

to achieve the university degree of

Diplom-Ingenieur

Master's degree programme: Biotechnology

submitted to

Graz University of Technology

Supervisor

Univ.-Prof. Dipl.-Ing. Dr.techn. Bernd Nidetzky

Institute of Biotechnology and Biochemical Engineering

Graz, December 20

AFFIDAVIT

I declare that I have authored this thesis independently, that I have not used other than the declared sources/resources, and that I have explicitly indicated all material which has been quoted either literally or by content from the sources used. The text document uploaded to TUGRAZonline is identical to the present master's thesis dissertation.

3.12.15
Date

Jan Braun
Signature

Abstract

The recently discovered Nitrile reductase QueF catalyzes the NADPH-dependent reduction of 7-cyano-7-deazaguanine ($preQ_0$) to 7-aminomethyl-7-deazaguanine ($preQ_1$), a late step in the bacterial biosynthetic pathway to the modified nucleoside queuosine (Q). It is the only known direct reduction of a nitrile to its corresponding primary amine and could expand the toolbox of biotechnologically usable nitrile modifying enzymes. This thesis addresses the effects of four different active site mutations at two critical positions on substrate binding, activity and side reactions of *E.coli* nitrile reductase QueF. The mutants C190A, C190S, D197A and D197H were studied using various methods like isothermal titration calorimetry (ITC), fluorescence quenching, HPLC and HPLC-MS. Both Cys190 and Asp197 were confirmed to play crucial roles in the catalytic mechanism, as neither substrate binding nor activity in mutants was comparable to wild type. Mutants with functional groups similar to wild type (C190S, D197H) were shown to be slightly but significantly more efficient than mutants with removed functionality (C190A, D197A) regarding substrate binding and nitrile reductase activity. Two unique side reactions involving the cofactor NADPH were discovered in the process and shown to be heavily influenced by the active site mutations: NADPH oxidation to $NADP^+$ by aerial oxygen and oxygen dependent NADPH degradation, which was especially enhanced by the D197A mutant.

Introduction

The recently discovered nitrile reductase QueF catalyzes the transformation of 7-cyano-7-deazaguanine ($preQ_0$) to 7-aminomethyl-7-deazaguanine ($preQ_1$), the only reduction of a nitrile group to its corresponding primary amine known in biology. The NADPH dependent reaction is part of the biosynthetic pathway present in bacteria leading to the modified nucleoside queuosine (Q) found in tRNA [1]. Two types of QueF, both belonging to the T-fold superfamily and showing sequence similarity to type I GTP cyclohydrolases (QueF was initially incorrectly annotated as cyclohydrolase), are currently known: the single-domain, homodecamer forming type I found in *Bacillus subtilis* and the two-domain, homodimer forming type II found in *E.coli* and *Vibrio cholerae*. Crystal structures were determined for both types of nitrile reductase QueF and N-glycosylase activity was proposed for *Vibrio cholerae* QueF [2, 3].

The development of a nitrile reductase as a versatile biocatalyst would expand the toolbox of available nitrile-degrading enzymes, previously consisting of nitrilases, nitrile hydratases, oxygenases and nitrogenases [4]. However, the kinetically sluggish reaction and stringent substrate specificity of QueF enzymes as well as the generally poor evolvability of T-fold enzymes pose challenges to the development and implementation of QueF nitrile reductases as useful biocatalysts for non-native substrates [5].

Based on the crystal structure of the type II nitrile reductase QueF, a catalytic mechanism was proposed involving three conserved amino acid residues in the active site: cysteine, aspartic acid and histidine (Cys190, Asp197 and His229 in the *E.coli* variant) [2, 5]. The proposed reaction is shown in Figure 1 and starts with the formation of a thioimidate intermediate as a result of the nucleophilic attack of the thiol group of Cys190 on the cyano group of the substrate $preQ_0$. The formation of this covalent enzyme-substrate adduct is followed by two subsequent steps of NADPH binding and hydride transfer from the NADPH molecules to the substrate, the first one leading to a thiohemiaminal intermediate and the second one leading to an imine, which finally collapses and releases the primary amine $preQ_1$. The reduction of a nitrile to its corresponding primary amine overall requires the transfer of two protons in addition to the two hydrides provided by NADPH. The first proton is transferred to the substrate during the initial formation of the covalent bond, the final proton is considered to be donated by His229. Asp197 is discussed to play an essential role in the formation of the covalent adduct by activating the thiol group of Cys190 via deprotonation and by then donating the initial proton to the nitrile nitrogen [6]. The section of the active site including

Cys190 and Asp197 and their relative positioning to $preQ_0$ and NADPH is shown in Figure 1. The catalytic mechanism has been compared to guanosine monophosphate (GMP) reductases, aldehyde dehydrogenases and UDP-glucose dehydrogenase, NAD(P)H dependent enzymes featuring a prominent nucleophilic cysteine residue and covalently bound reaction intermediates [5, 7–9].

All QueF enzyme variants described so far exhibit very stringent substrate specificity. QueF enzymes from different sources were characterized regarding their substrate spectrum and showed no catalytic activity towards simple, commercially available nitriles and either no or significantly decreased catalytic activity towards analogues of the natural substrate [5, 10, 11]. The conserved active site amino acids Cys190 and Asp197 were reported to be essential for the catalytic mechanism. Mutations at these positions lead to practically inactive enzymes (<0.001% of wild-type activity for C55A/C55S of *Bacillus subtilis* QueF) or complete loss of activity (C190A, D197N) [10–12]

Here, we wish to report effects of different mutations at the most critical positions of the *E.coli* nitrile reductase QueF. The active site nucleophile Cys190 was replaced by alanine, removing the functional group, and by serine, providing another nucleophile to the active site. The Asp197 residue was replaced by alanine, removing the functional group, and by histidine in an attempt to recover some of the proton acceptor/donor functionality of the aspartic acid. Since both positions of interest are considered to be prominently involved in substrate binding, interaction of the mutant enzymes with the substrate $preQ_0$ was investigated using different approaches. Furthermore, the residual activity of the different mutants towards $preQ_0$ as well as possible interactions and side reactions involving the co-factor NADPH were determined. Significant differences between individual mutants were analyzed and possible explanations were examined in context with the proposed mechanism in an attempt to elucidate the roles of Cys190 and Asp197 in substrate and cofactor binding and catalytic activity.

Results & Discussion

Preparation of mutant enzyme

The mutagenesis, protein expression and protein purification protocols described in the experimental section were successfully applied to create C190S, D197A and D197H mutant and wild type enzyme (C190A mutagenesis done by Wildling et al. [11]). No significant

difference between individual mutants could be determined regarding expression efficiency and enzyme purity.

Enzyme-substrate interaction

Photometric analysis of adduct formation

Formation of a covalent thioimidate intermediate between enzyme and substrate, evidenced by an absorbance maximum at 376 nm, was shown for wild type enzyme, but for neither mutant enzyme. The measured spectra for wild type and D197H mutant enzyme with and without the substrate $preQ_0$ are shown in Figure 2. This proves an essential role of both Cys190 and Asp197 for formation of the covalent adduct and confirms the findings of Lee et al. [12] for wild type and cysteine mutants, but has not been shown before for aspartic acid mutants. Different pH and chemical rescue agents did not have a significant effect.

Protein-MS

Masses correlating to a stable adduct between enzyme and substrate were found for wild type and D197H mutant enzyme (Table 1), but for neither of the other mutants. The ratio of enzyme-substrate complex to free enzyme was calculated based on the relative abundances shown in Table 1 and is significantly higher for wild type (≈ 57 % of enzyme bound to substrate) compared to D197H (≈ 21 % of enzyme bound to substrate), suggesting more efficient substrate binding for wild type enzyme. This result seems to contradict the inability of D197H to form a covalent adduct with the substrate, as only covalent bonds are expected to be stable enough to persist through the MS procedure. The amount of substrate bound enzyme determined with protein-MS is also clearly above the detection limit of the photometric analysis for covalent adduct. However, it has been shown previously that the active site closes around and thereby tightly binds the substrate once contact is made, and that this closure is not caused by formation of the covalent bond [3]. The available data suggests that D197H is the only analyzed mutant that interacts with the substrate strong enough to trigger active site closure, forming a stable, non-covalent enzyme-substrate complex.

Tryptophane quenching

Significant reduction of fluorescence intensity due to substrate addition could be observed for wild type and all mutants. Fluorescence quenching was much too strong in all cases to be consistent with collisional quenching [13], indicating static quenching and therefore interaction with the substrate. The calculated Stern-Volmer constants for the individual

mutants (Table 2 and Figure 2) suggest that quenching was generally stronger for aspartic acid mutants compared to cysteine mutants, whereas mutants with functional groups (C190S, D197H) showed a larger effect compared to mutants with removed functionality (C190A, D197A). D197H exhibited an approximately tenfold higher Stern-Volmer constant (K_{SV}) compared to the other mutants. The fluorescence spectra and the Stern-Volmer analysis for mutant D197H are shown in Figure 2. However, neither mutant had a Stern-Volmer constant in the range of the wild type, indicating a distinctly stronger interaction of wild type enzyme with the substrate. Different pH and chemical rescue agents did not have a significant effect on tryptophane quenching

Isothermal titration calorimetry (ITC)

Results of isothermal titration calorimetry (Figure 3) indicate interaction between enzyme and substrate for wild type and all mutants. Dissociation constant (K_D) and Gibb's free energy (ΔG), the main parameters for overall binding efficiency and affinity, were far more in favor of binding (i.e. low K_D and negative ΔG) for wild type compared to all mutants and only wild type showed a sigmoid curve typical for integrated ITC data. While K_D and ΔG were in the same range for all mutants, both indicated slightly stronger affinity to substrate for mutants with functional groups (C190S, D197H) compared to mutants with removed functionality (C190A, D197A). There was a more distinct difference between mutants regarding reaction enthalpy (ΔH) and reaction entropy (ΔS), with ΔH clearly more in favor of binding for aspartic acid mutants (D197A, D197H) and ΔS clearly more in favor of binding for cysteine mutants (C190A, C190S). ΔH for wild type was in the same range as for aspartic acid mutants, while ΔS had very little influence on binding thermodynamics of wild type enzyme. When interpreting thermodynamic binding data for enzyme-substrate interactions, favorable ΔH values are attributed to specific noncovalent interactions (e.g. hydrogen bonding or van der Waals contacts) and favorable ΔS values to hydrophobic interactions and favorable desolvation [14]. ITC results accordingly indicate affinity mainly dominated by specific interactions for aspartic acid mutants and by hydrophobic interactions and solvation effects for cysteine mutants, while affinity for wild type almost exclusively stems from hydrogen and covalent bonds. This confirms Cys190 as the residue mainly responsible for specific interaction with the substrate, as mutants at that position exhibit significantly lower specific affinity compared to wild type and other mutants.

Nitrile reduction and NADPH degradation

HPLC

Average formation and consumption rates of all reaction components were determined by HPLC as described in the experimental section and are shown in Table 3. As expected from studies of cysteine and aspartic acid mutants in literature [11,12], all analyzed mutants exhibit drastically reduced nitrile reductase activity compared to wild type enzyme (0.002% - 0.02 % of wild type). However, significant differences are evident between cysteine mutants and aspartic acid mutants, with cysteine mutants being more active, and between mutants with and without functional groups, with functional groups leading to more activity. C190S is 1.5 times more active than C190A and D197H is nearly 4 times more active than D197A. The typical course of $preQ_1$ concentration over a 96 h reaction for each mutant is shown in Figure 4. The possibility of measured activity being present due to wild type contamination was considered but is improbable, as differences between individual mutants are reproducible over multiple batches of enzyme production. Similar mutagenesis studies were conducted with the aforementioned cysteine containing enzymes GMP reductase, aldehyde dehydrogenase and UDP-glucose dehydrogenase. While comparatively high residual activity (> 5% of wild type [7]) with removed cysteine nucleophile was reported for GMP reductase, measured activities for cysteine to serine mutants of aldehyde dehydrogenase (0.007 % of wild type [8]) and UDP-glucose dehydrogenase (< 0.01 % of wild type [15]) were similar to the C190S mutant of nitrile reductase QueF. This suggests an even more substantial role of the cysteine residue for nitrile reductases, aldehyde dehydrogenases and UDP-glucose dehydrogenases compared to GMP reductases. UDP-glucose dehydrogenase was still able to form a covalent intermediate with the cysteine replaced with serine, which has not been shown for any of the other enzymes. Two side reactions involving NADPH were detected: Degradation of NADPH to products later identified by HPLC-MS and oxidation of NADPH to $NADP^+$ with no apparent electron acceptor. To further investigate the side reactions and compare mutant enzyme to wild type in this regard, reaction mixtures without $preQ_0$ were analyzed (Table 4). Typical courses of side reaction product concentrations over a 24 h reaction for each mutant are shown in Figure 4. Both side reactions were shown to be oxygen dependent as none was present under anaerobic conditions (Figure 5), suggesting an oxygen dependent degradation mechanism and aerial oxygen as electron acceptor. Side reactions are present in control reactions without enzyme, but heavily influenced by the presence of enzyme. NADPH degradation is accelerated by wild type and aspartic acid mutants, especially D197A. Possible

explanation for this behavior lies in the structural similarity between the substrate $preQ_0$ and the cofactor NADPH, as both possess two membered nitrogen heterocycles. Interaction between NADPH and the substrate binding pocket of the enzyme instead of the original NADPH binding pocket, leading to positioning of NADPH in a more reactive form favoring degradation is conceivable. Increased affinity of D197A mutant enzyme to NADPH could be explained by the exchange of the bulky aspartic acid with the small alanine leading to additional space in the vicinity of the active site and possibly less stringent binding specificity. The absence of increased NADPH degradation in reactions with cysteine mutants suggests a crucial role of the cysteine residue in NADPH binding and the degradation mechanism. NADPH oxidation by aerial oxygen is accelerated by wild type and all analyzed mutants except D197A. Similar rates were determined for C190A, C190S and D197H, while the strongly increased NADPH degradation in D197A probably leads to apparent absence of the other side reaction. Both NADPH degradation and oxidation are decelerated in presence of $preQ_0$, probably due to competition between substrate and cofactor for the binding pocket. Different pH and chemical rescue agents did not have a significant effect on nitrile reductase activity and side reactions.

HPLC-MS

The identities of the nitrile reduction product $preQ_1$ and of two NADPH degradation products were successfully confirmed by HPLC-MS as described in the experimental section. The masses found for NADPH degradation products (m = 761 Da, m = 639 Da, Figure 5) fit the masses found by Hofmann et al. [16] and confirm the proposed oxygen dependent degradation pathway, an oxidative ring opening of the furanose ring and subsequent cleavage of the nicotinamide (Figure 5). N-glycosylase activity of QueF and possible impact on the N-glycosyl bond in NADPH have already been reported and discussed in literature, but have never been further investigated or linked to active site mutations before. Kim et al. [2] discussed a possible mechanism, with His229 and Arg258 as key residues (His233 and Arg262 in the *Vibrio cholerae* variant). Their crystal structure suggests that both residues could be in position for proton donation to the nitrogen containing heterocycle and to facilitate the cleavage of the N-glycoside bond. Our data clearly indicates a big influence of active site mutations, especially at the Asp197 position, on this mechanism.

Conclusions

Analysis of enzyme-substrate interaction using different methods confirmed both Cys190 and Asp197 are crucial residues for substrate binding, as all mutations at these positions lead to loss of ability to form covalent thioimidate intermediates and drastically reduced interaction and binding efficiency. This verifies the research that has been done on cysteine mutants and speaks for the presumed role of Asp197 in substrate binding as proton acceptor and activator of Cys190 and as proton donor to the substrate nitrile group. However, residual interaction was found for all mutants and inserting functional groups similar to wild type at both positions was shown to have a positive effect on substrate binding, as both C190S and D197H showed stronger interaction and more efficient substrate binding than C190A and D197A, respectively. Results from different methods indicate that from the analyzed mutants D197H is not only exhibiting the strongest interaction with substrate, but is also the only mutant undergoing the same conformational changes upon substrate binding as wild type enzyme.

Measured activities of individual QueF mutants on $preQ_0$ confirm the crucial role of Cys190 and Asp197 in the catalytic mechanism and are consistent with substrate binding analysis. Very little activity could be restored by introduction of mutations similar to wild type at said positions without reaching more than 0.02 % of wild type activity. Mutations at Cys190 and Asp197 also had strong effects on two oxygen dependent side reactions involving NADPH, of which the NADPH degradation was already discussed, but never linked to active site mutations in literature.

Experimental procedures

General

All reagents with exception of $preQ_0$ (synthesis procedure given in [10]), which was provided by Norbert Klempier (Graz University of Technology) were bought from commercial suppliers. The dNTPs for PCRs and the DpnI restriction enzyme were from Thermo Scientific (USA). Pfu DNA Polymerase and its reaction buffer were from Promega (USA). NADPH (purity $\geq$ 97 %), sodium phosphates and all chemicals used in media for enzyme expression and in buffers for enzyme purification, storage and reactions were from Carl Roth (Germany). IPTG, tetrabutylammonium bisulfate and dibutylammonium acetate were from Sigma-Aldrich (USA). Ammonium acetate was from Merck (Germany). Acetonitrile was from Chemlab (Belgium)

Preparation of mutant enzyme

Site specific mutagenesis

The pEHISTEV vector carrying the wild type sequence of *E.coli* nitrile reductase (pEHISTEV_EcNRedWT) [11, 17] was employed as the template for a two-stage, PCR driven site specific mutagenesis protocol. The following primers were ordered from IDT and used for the mutagenesis: C190S fw 5' CTG AAA TCA AAC AGC CTG ATC ACC C 3', C190S rv 5' GGT TGA TGG GTG ATC AGG CTG TTT GAT TT 3', D197A fw 5' CCT GAT CAC CCA TCA ACC AGC GTG GGG T 3', D197A rv 5' GGA GCG AAC CCC ACG CTG GTT GAT GGG T 3', D197H fw 5' CCT GAT CAC CCA TCA ACC ACA TTG GGG TT 3', D197H rv 5' GGA GCG AAC CCC AAT GTG GTT GAT GGG T 3'. The two step PCR was carried out on an Applied Biosystems 2720 thermal Cycler. In the first step, a reaction of 10 µL template vector (100 ng/µL), 1 µL dNTP mix (10 mM each), 1.5 µL either forward or reverse primer (10 µM), 5 µL Pfu DNA Polymerase Reaction Buffer (10x), 1 µL Pfu DNA Polymerase (3 U/µL) and 31.5 µL ddH_2O was subjected to the following temperature program: 1 min 95°C initial denaturation, 4 cycles of 50 s 95°C, 50 s 55°C, 10 min 70°C and 7 min 70 °C final elongation. For the second step, 25 µL of the reaction containing the forward primer were combined with 25 µL of the reaction containing the respective reverse primer and an additional 18 cycles were run under the above conditions. DpnI (1 µL, 10 U/µL) was added and the template DNA was digested for 2 h at 37 °C. Aliquots (2 µL) of the resulting mixture were transformed into electrocompetent *E.coli* Bl21 (DE3) cells with a 2.5 kV pulse using a Bio-Rad Micropulser. SOC medium (1 mL) was added immediately after transformation, cells were regenerated for 2 h at 37°C and 50 µL aliquots were plated on LB/kanamycine agar plates (10 g/L peptone from casein, 5 g/L yeast extract, 5 g/L NaCl, 50 mg/L kanamycine-sulfate, 30 g/L agar) to select positive transformants. Correct mutations were confirmed by the sequencing service of LGC Genomics. The C190A mutant was produced and provided by Wildling et al. [11]

Enzyme expression and purification

Cultivation was carried out in a in a Sartorius Certomat BS-1 shaker as follows: *E.coli* Bl21 (DE3) pEHISTEV_EcNRed seed cultures containing wild type and different mutants were grown in 50 mL LB/kanamycine media (10 g/L peptone from casein, 5 g/L yeast extract, 5 g/L NaCl, 50 mg/L kanamycine-sulfate, 30 g/L agar) in 300 mL baffled shaking flasks for 18 h at 37 °C and 110 rpm. Main cultures (250 mL LB/kanamycine media in 1 L baffled shaking flasks) were inoculated with 5 mL of respective seed culture and grown at 37 °C and 110 rpm

to an OD_{600} of approximately 0.7, measured on a Beckmann Coulter DU 800 photometer in Sarstedt cuvettes. The cultures were then induced with a final concentration of 1 mM IPTG and grown for 22 h at 25 °C and 120 rpm. Cells were harvested by 25 min centrifugation at 5000 rpm and 4 °C in a Sorvall Evolution RC 3000 centrifuge. The pellets were resuspended in 5 mL 0.9 % NaCl, followed by a 60 min centrifugation step at 5000 rpm and 4 °C in an Eppendorf 5804 R centrifuge and resuspension in 5 mL enzyme storage buffer (100 mM Tris-HCl, 50 mM KCl, 1 mM TCEP, 1% glycerol, pH 7.5) The cells were disrupted by ultra-sonication using a Sonics & Materials Vibra Cell sonicator and cell debris was removed by 20 min centrifugation in an Eppendorf 5415 R micro centrifuge at 16 000 rpm and 4 °C. The enzyme was purified from the cell free extract using GE Healthcare HisTrap protein purification columns and a GE Healthcare ÄKTAPrime Plus chromatography system. The following protocol was applied: The column was washed with 100 % equilibration buffer (50 mM Tris-HCl, 100 mM NaCl, 3 mM EDTA, 1 mM DTT, 10 mM imidazole, pH 7.4) at 5 mL/min for 10 min. The cell free extract was loaded to the column manually with a syringe and unspecifically bound protein was washed away with 100 % equilibration buffer at 5 mL/min for 10 min. The target protein was eluted with 60 % equilibration buffer and 40 % elution buffer (50 mM Tris-HCl, 100 mM NaCl, 3 mM EDTA, 1 mM DTT, 500 mM imidazole, pH 7.4) at 5 mL/min for 20 min with the automatic fraction collector on. All solvents used for purification were filtered using a Sartorius cellulose acetate filter (0.45 µm). Separate columns were used for individual mutants to avoid cross-contaminations. Protein containing fractions were pooled and rebuffered to enzyme storage buffer with GE Healthcare PD-10 desalting columns. Protein concentration was determined with the Pierce BCA protein Assay Kit from Thermo Scientific and increased to 60-100 mg/mL using Vivaspin 20 columns (10 000 MWCO, Sartorius). The purity of the enzyme preparations was confirmed by SDS-PAGE, using Invitrogen NuPAGE Novex 4-12 % Bis-Tris Protein Gels. The enzymes were stored at -20 °C and used within 4 weeks after purification.

Enzyme-substrate interaction

Photometric analysis of adduct formation

Formation of the covalent thioimidate adduct was confirmed using a Beckmann Coulter DU 800 photometer and Sarstedt cuvettes. Enzyme (50 µM, no enzyme in control sample) was mixed with substrate ($preQ_0$, 250 µM) in reaction buffer (100 mM Tris-HCl, 50 mM KCl, 1.15 mM TCEP, pH 7.5, also 1% DMSO due to substrate solvation) and an absorbance

wavelength scan (300-500 nm) was conducted with pure reaction buffer as blank. In addition to the standard reaction buffer, buffer with pH 6 and pH 9 as well as buffer supplemented with either sodium azide (100 mM) sodium formate (100 mM) or sodium acetate (100 mM) was used.

Protein-MS

Enzyme (130 µM) was mixed with substrate (500 µM) protein-MS buffer (50 mM Tris-HCl, 50 mM KCl, 1 mM TCEP, pH 7.5, also 1% DMSO due to substrate solvation) and the solution was desalted using Amicon Ultra 0.5 mL Centrifugal filter units (Millipore, Billerica, US). A final protein concentration of 30 pmol/µL was obtained with water containing 5 % acetonitrile (ACN) and 0.1 % trifluoracetic acid (TFA). Two different methods of protein separation and detection were applied. For analysis of wild type and mutant enzyme, the separation of possible protein variants was carried out on a 1200 Agilent capillary HPLC system using a Thermo PepSwift RP monolithic column (50 x 0.5 mm) at a flow rate of 20 µL/min and a column temperature of 60 °C. The gradient of solution A (water + 0.05 % TFA) and B (ACN + 0.05 % TFA) was performed as follows: 10 % B for 5 min, 10 – 100 % B for 50 min, 100 % - 10 % B for 1 min, 10 % B for 15 min. Injection volume was 5 µL. The Thermo Fisher Scientific LTQ-FT mass spectrometer was operated with an ESI source in positive mode with following settings: mass range: 300 – 2000 m/z, resolution 400 000, 500 ms injection time, 1 microscan, source voltage 5 kV, capillary voltage 35 V, sheath gas flow 15. The protein mass spectra were deconvoluted by the Thermo Fisher Scientific software Protein Deconvolution 2.0, using the Xtract algorithm. The following main parameters were applied: charge carrier, H^+, m/z range, min. 800 to max. 2000, min. detected charge state, 4, s/n threshold, 5, rel. abundance threshold, 20 %. For further analysis of the D197H mutant, the separation of possible protein variants was carried out on a Dionex capillary HPLC system using a Thermo PepSwift RP monolithic column (50 x 0.5 mm) at a flow rate of 15 µL/min and a column temperature of 60 °C. The gradient of solution A (water + 0.3 % FA) and B (ACN + 0.3 % FA) was performed as follows: 10 % B for 5 min, 10 – 100 % B for 50 min, 100 % - 10 % B for 1 min, 10 % B for 15 min. Injection volume was 5 µL. The Bruker maXis II ETD mass spectrometer was operated with the captive spray source in positive mode with following settings: mass range: 250 – 3000 m/z, 1 Hz, source voltage 1.6 kV, dry gas flow 3L/min with 180 °C. The protein mass spectra were deconvoluted by the Data analysis software, using the MaxEnt2 algorithm. The following main parameters were applied: charge carrier, H+, m/z range, min. 800 to max. 2000, min. instrument resolving power was set to

50.000. For peak detection SNAP algorithm with following parameters were used: Quality factor threshold 0.9, S/N threshold 2 and maximum charge state of 12.

Tryptophane quenching

Quenching of tryptophane based fluorescence as result of enzyme-substrate ($preQ_0$) interaction was analyzed using a Hitachi F-4500 fluorescence photometer and Hellma Analytics UV precision cuvettes. Enzyme (2.8 µM) was mixed with either 0, 3, 7.5, 15 or 30µM substrate in reaction buffer and the resulting fluorescence was analyzed using the following parameters: excitation wavelength 280 nm, emission wavelength scan 300-500 nm. Emission at a wavelength of 330 nm was used to calculate the Stern-Volmer constant for wild type enzyme and each individual mutant using the Stern-Volmer equation [13]. Buffer with different pH (pH 6, and pH 9) and different supplements (Na-azide, Na-formate, Na-acetate) was used in addition to standard reaction buffer as mentioned before.

Isothermal titration calorimetry

Thermodynamics of the enzyme-substrate ($preQ_0$) affinity as well as enzyme-cofactor (NADPH) affinity was analyzed by isothermal titration calorimetry using a Malvern Microcal VP-ITC system. Briefly, this system is able to measure the change in enthalpy when small volumes of one interaction partner are injected to a solution of a second interaction partner. Thus, thermodynamic parameters of the interaction between biomolecules can be determined [18]. The following parameters were applied: 28 total injections, 6 µL injection volume, 12 s injection duration, 300 s injection spacing, 25 °C temperature, 800 µM syringe concentration (substrate in reaction buffer), 45 µM cell concentration (enzyme in reaction buffer, pure reaction buffer for reference sample). When analyzing cofactor affinity, 500 µM syringe concentration (NADPH) and 35 µM cell concentration (enzyme) were used. Standard reaction buffer as described before was used as solvent for enzyme, substrate and cofactor solutions.

Nitrile reduction and NADPH degradation

HPLC

Concentration of substrate ($preQ_0$), product ($preQ_1$), NADPH, $NADP^+$, and NADPH degradation products during incubation with enzyme was measured on an Agilent 1200 series HPLC system. Two different columns and time profiles were used. For a Merck SeQuant ZIC HILIC Analytical PEEK 250-2.1 column (5 µm particle diameter, 200 Å pore size), 5 µL sample were injected and a 20 min gradient starting at 20 % running buffer (20 mM

ammonium acetate, pH 6.67)/ 80 % acetonitrile and finishing at 40 % running buffer/60% acetonitrile with 0.5 mL/min flow rate was applied. For a Merck Cromolith High Resolution RP-18 endcapped 100-4.6 column, 20 µL sample were injected and a 10 min gradient starting at 95 % running buffer (50 mM sodium phosphate, pH 6.8 + 2 mM tetrabutylammonium bisulfate)/5 % acetonitrile and finishing at 84 % running buffer/16 % acetonitrile with 2 mL/min flow rate was applied. Absorbance at 254 nm and 340 nm was measured in both methods. All solvents used on the HPLC system were filtered using a Sartorius cellulose acetate filter (0.45 µm). Enzyme (50 µM, no enzyme in control sample) was mixed with either substrate ($preQ_0$, 250 µM) + NADPH (500 µM) or only with NADPH (500 µM) in reaction buffer and incubated at 25 °C and 500 rpm at an Eppendorf Thermomixer Comfort. Buffer with different pH (pH 6 and pH 9) and different supplements (Na-azide, Na-formate, Na-acetate) was used in addition to standard reaction buffer as mentioned before. In addition to the standard incubation, reaction mixtures were also incubated under anaerobic conditions using a Plas Labs controlled atmosphere chamber. Calibration curves for all substances were produced using standards containing 500 µM, 400 µM, 300 µM, 200 µM and 100 µM of the particular compound. Samples were taken after 0 h, 1 h, 3 h, 6 h, 24 h, 48 h, 72 h and 96 h according to the following procedure: Reaction mixture (50 µL) was added to acetonitrile (100 µL) and incubated 15 min on ice, followed by 15 min centrifugation at 16 000 rpm and 4 °C in an Eppendorf 5415 R micro centrifuge. The supernatant was directly injected to the HPLC system for the ZIC HILIC method and diluted four fold with the respective running buffer before injection for the Cromolith method.

HPLC/MS

Identity of nitrile reduction product ($preQ_1$) and NADPH degradation products was confirmed on an Agilent HPLC 1200 series HPLC system coupled with an Agilent G1956B MSD mass detector. The ZIC-HILIC method was applied as described in the HPLC section, additionally using Single Ion Monitoring (SIM) at an m/z of 180 to confirm the presence of $preQ_1$. The Cromolith method was adapted for HPLC/MS by using a 20 min gradient starting at 90 % running buffer (5 mM dibutylammonium acetate, pH 6.8)/10 % acetonitrile and finishing at 80 % running buffer/20 % acetonitrile with 1 mL/min flow rate. A mass scan covering an m/z range of 50-900 was conducted to identify unknown NADPH degradation products. Sample preparation was conducted as described in the HPLC section.

Acknowledgements:

This work was supported by the Federal Ministry of Economy, Family, and Youth (BMWFJ), the Federal Ministry of Traffic, Innovation, and Technology (BMVIT), the Styrian Business Promotion Agency (SFG), the Standortagentur Tirol, and ZIT—the Technology Agency of the City of Vienna through the COMET Funding Programme managed by the Austrian Research Promotion Agency FFG. The authors gratefully acknowledge Norbert Klempier (Graz University of Technology) for provision of $preQ_0$, Ruth Birner-Grünberger (Medical University of Graz) for protein-MS analysis and Birgit Wiltschi (Graz University of Technology, acib GmbH) and Norbert Klempier (Graz University of Technology) for HPLC-MS analysis.

Author contributions:

[JB] planned and performed the experiments, analyzed the data and wrote the paper. [JJ] planned and performed the experiments. [TC] planned the experiments and analyzed the data. [BN] planned the experiments and wrote the paper. All authors have read and approved the paper.

References

1. van Lanen SG, Reader JS, Swairjo MA, Crécy-Lagard V de, Lee B & Iwata-Reuyl D (2005). From cyclohydrolase to oxidoreductase: discovery of nitrile reductase activity in a common fold. *Proceedings of the National Academy of Sciences of the United States of America* **102,** 4264–4269.

2. Kim Y, Zhou M, Moy S, Morales J, Cunningham MA & Joachimiak A (2010). High-resolution structure of the nitrile reductase QueF combined with molecular simulations provide insight into enzyme mechanism. *Journal of molecular biology* **404,** 127–137.

3. Chikwana VM, Stec B, Lee BWK, Crécy-Lagard V de, Iwata-Reuyl D & Swairjo MA (2012). Structural basis of biological nitrile reduction. *The Journal of biological chemistry* **287,** 30560–30570.

4. Banerjee A, Sharma R & Banerjee UC (2002). The nitrile-degrading enzymes: current status and future prospects. *Applied microbiology and biotechnology* **60,** 33–44.

5. Yang L, Koh SL, Sutton PW & Liang Z (2014). Nitrile reductase as a biocatalyst. *Catal. Sci. Technol.* **4,** 2871.

6. Ribeiro AJM, Yang L, Ramos MJ, Fernandes PA, Liang Z & Hirao H (2015). Insight into Enzymatic Nitrile Reduction. *ACS Catal.* **5,** 3740–3751.

7. Li J, Wei Z, Zheng M, Gu X, Deng Y, Qiu R, Chen F, Ji C, Gong W, Xie Y & Mao Y (2006). Crystal structure of human guanosine monophosphate reductase 2 (GMPR2) in complex with GMP. *Journal of molecular biology* **355,** 980–988.

8. Cobessi D, Tête-Favier F, Marchal S, Branlant G & Aubry A (2000). Structural and biochemical investigations of the catalytic mechanism of an NADP-dependent aldehyde dehydrogenase from Streptococcus mutans. *Journal of molecular biology* **300,** 141–152.

9. Campbell RE, Sala RF, van de Rijn I & Tanner ME (1997). Properties and Kinetic Analysis of UDP-glucose Dehydrogenase from Group A Streptococci. *Journal of Biological Chemistry* **272,** 3416–3422.

10. Wilding B, Winkler M, Petschacher B, Kratzer R, Glieder A & Klempier N (2012). Nitrile Reductase from Geobacillus kaustophilus. *Adv. Synth. Catal.* **354,** 2191–2198.

11. Wilding B, Winkler M, Petschacher B, Kratzer R, Egger S, Steinkellner G, Lyskowski A, Nidetzky B, Gruber K & Klempier N (2013). Targeting the substrate binding site of E. coli

nitrile reductase QueF by modeling, substrate and enzyme engineering. *Chemistry (Weinheim an der Bergstrasse, Germany)* **19,** 7007–7012.

12. Lee BWK, van Lanen SG & Iwata-Reuyl D (2007). Mechanistic studies of Bacillus subtilis QueF, the nitrile oxidoreductase involved in queuosine biosynthesis. *Biochemistry* **46,** 12844–12854.

13. Lakowicz JR (2010) Principles of fluorescence spectroscopy, 3rd edn. Springer, New York, NY.

14. Núñez S, Venhorst J & Kruse CG (2012). Target-drug interactions: first principles and their application to drug discovery. *Drug discovery today* **17,** 10–22.

15. Ge X, Campbell RE, van de Rijn I & Tanner ME (1998). Covalent Adduct Formation with a Mutated Enzyme. *J. Am. Chem. Soc.* **120,** 6613–6614.

16. Hofmann D, Wirtz A, Santiago-Schübel B, Disko U & Pohl M (2010). Structure elucidation of the thermal degradation products of the nucleotide cofactors NADH and NADPH by nano-ESI-FTICR-MS and HPLC-MS. *Analytical and bioanalytical chemistry* **398,** 2803–2811.

17. Liu H & Naismith JH (2009). A simple and efficient expression and purification system using two newly constructed vectors. *Protein expression and purification* **63,** 102–111.

18. Freire E, Mayorga OL & Straume M (1990). Isothermal titration calorimetry. *Anal. Chem.* **62,** 950A-959A.

Tables

Table 1: Results of the protein-MS analysis of wild type and D197H mutant nitrile reductase QueF with substrate $preQ_0$. The difference (dM) between expected masses (m/z_{exp}) and detected masses (m/z_{det}) was calculated and relative abundances (RA) of detected masses were determined.

	m/z_{exp}[Da]	m/z_{det} [Da]	dm [Da]	RA [%]
Wild type (free enzyme)	35 732.64	35 732.11	0.53	74.61
Wild type (enzyme-substrate complex)	35 907.69	35 906.03	1.66	100
D197H (free enzyme)	35 754.68	35 755.88	1.20	100
D197H (enzyme-substrate complex)	35 929.72	35 927.90	1.82	26.45

Table 2: Stern-Volmer constant (K_{SV}) for wild type and mutant QueF

	K_{SV} [M^{-1}]
Wild type	1.69×10^6
C190A	1.62×10^4
C190S	4.17×10^4
D197A	5.33×10^4
D197H	2.71×10^5

Table 3: Average rates of $preQ_1$, $NADP^+$ and NADPH degradation product formation and $preQ_0$ and NADPH consumption in reactions with mutant QueF, substrate ($preQ_0$) and cofactor (NADPH)

	preQo [µM/h]	$preQ_1$ [µM/h]	NADPH [µM/h]	$NADP^+$ [µM/h]	Degradation products [µM/h]
Control	0.056 (± 0.025)	0	3.3 (± 0.20)	0.37 (± 0.0081)	3.0 (± 0.40)
C190A	0.59 (± 0.077)	0.45 (± 0.0073)	4.3 (± 0.63)	1.7 (± 0.16)	2.1 (± 0.36)
C190S	0.73 (± 0.042)	0.68 (± 0.0077)	4.6 (± 0.31)	2.1 (± 0.18)	2.0 (± 0.40)
D197A	0.11 (± 0.011)	0.087 (± 0.026)	43 (± 3.1)	0.61 (± 0.044)	39 (± 4.3)
D197H	0.33 (± 0.037)	0.30 (± 0.035)	8.4 (± 1.4)	2.6 (± 0.55)	5.8 (± 0.042)

Table 4: Average rates of $NADP^+$ and NADPH degradation product formation and NADPH consumption in reactions with wild type or mutant QueF and cofactor (NADPH)

	NADPH [µM/h]	$NADP^+$ [µM/h]	Degradation products [µM/h]
Control	4.1	0.39	3.9
Wild Type	11	4.2	6.8
C190A	3.8	2.4	1.9
C190S	4.7	2.5	2.2
D197A	200	0.53	200
D197H	11	4.8	6.5

Figures

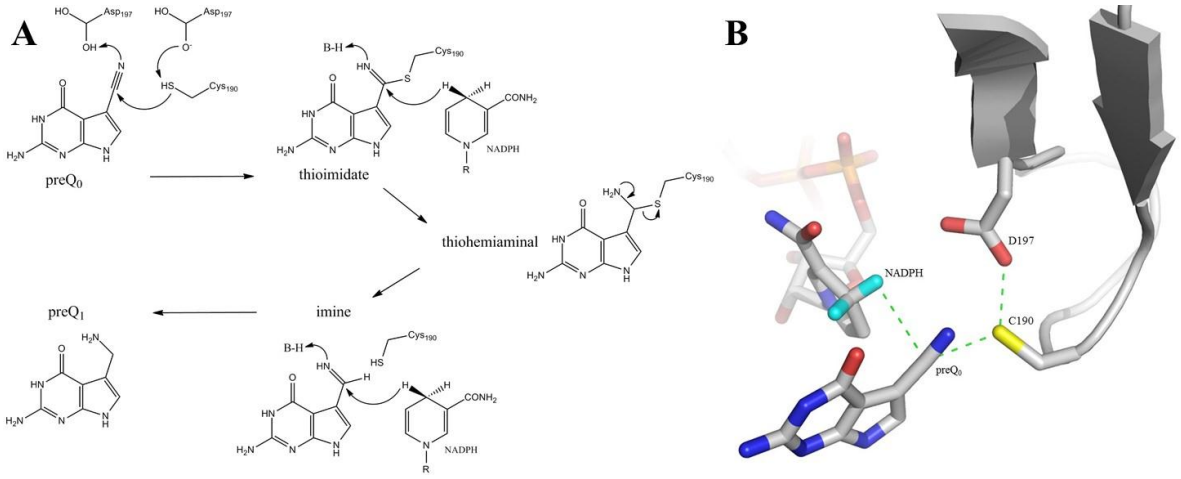

Figure 1: ***A****: Proposed reaction mechanism of nitrile reductase QueF.* ***B****: Active site of nitrile reductase QueF with residues Cys190 and Asp197, substrate $preQ_0$ and cofactor NADPH. Green dashed lines indicate crucial intertactions.*

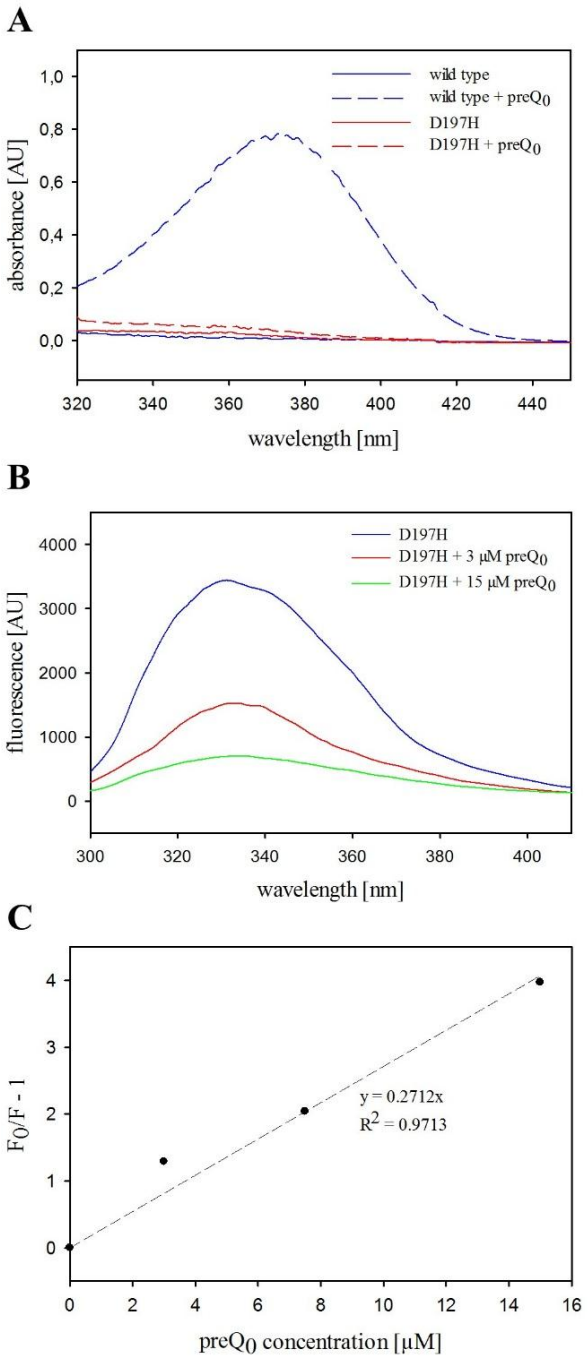

Figure 2: Results of the enzyme-substrate interaction analysis of nitrile reductase QueF ***A****: Photometric spectra of wild type and D197H mutant enzyme (50 µM) with and without substrate (250 µM). Absorbance maximum at 376 nm indicates covalent enzyme-substrate complex.* ***B****: Fluorescence spectra of D197H mutant enzyme (2.8 µM) with 0, 3, 7.5 and 15 µM substrate. Decreasing fluorescence indicates enzyme substrate interaction.* ***C****: Stern-Volmer analysis for D197H mutant enzyme. F_0 = fluorescence in absence of substrate, F = fluorescence in presence of substrate. Slope of the regression curve equals Stern-Volmer constant (K_{SV})*

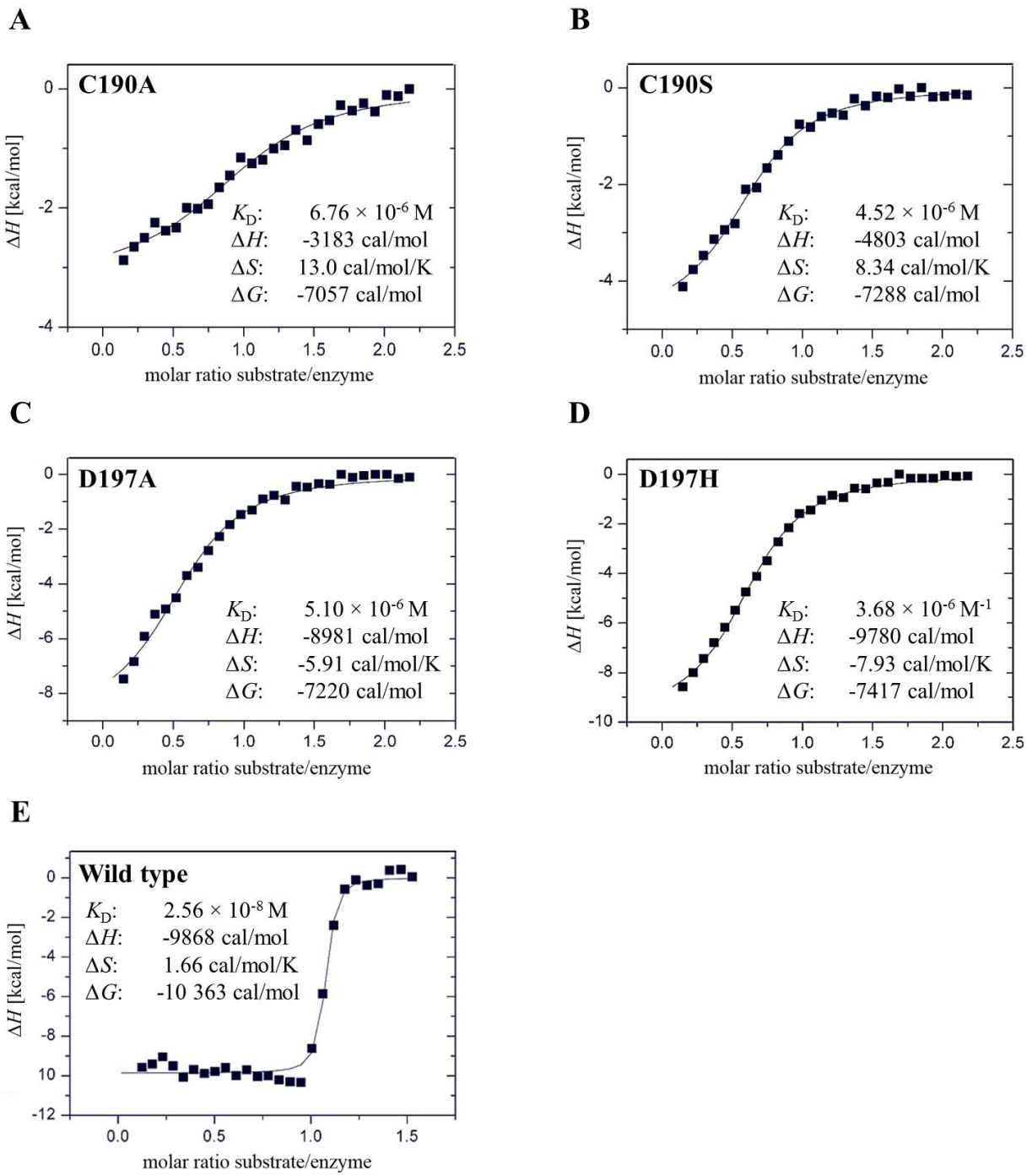

Figure 3: Results of isothermal titration calorimetry for wild type and mutant nitrile reductase QueF. Each square represents ΔH for a single injection of 6 µl preQ$_0$ solution (800 µM) into enzyme solution (45 µM). Calculated parameters: Dissociation constant (K_D) reaction enthalpy (ΔH), reaction entropy (ΔS) and Gibb's free energy (ΔG). ***A****: C190A* ***B****: C190S* ***C****: D197A* ***D****: D197H* ***E****: wild type*

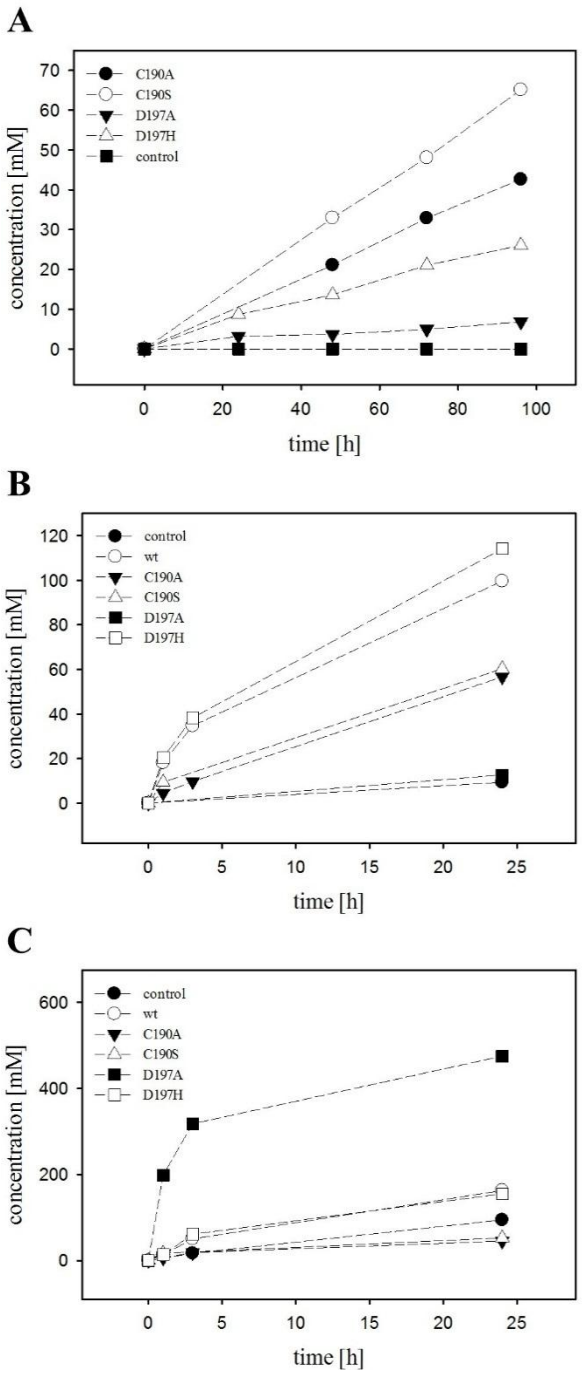

Figure 4: Typical courses of reactions with nitrile reductase QueF wild type and active site mutants. ***A****: Course of preQ$_1$ concentration over a 96 h reaction with enzyme (50 µM), substrate (preQ$_0$, 250 µM) and cofactor (NADPH, 500 µM).* ***B****: Course of NADP$^+$ concentration over a 24 h reaction with enzyme (50 µM) and cofactor (NADPH, 500 µM).* ***C****: Course of NADPH degradation product concentration over a 24 h reaction with enzyme (50 µM) and cofactor (NADPH, 500 µM).*

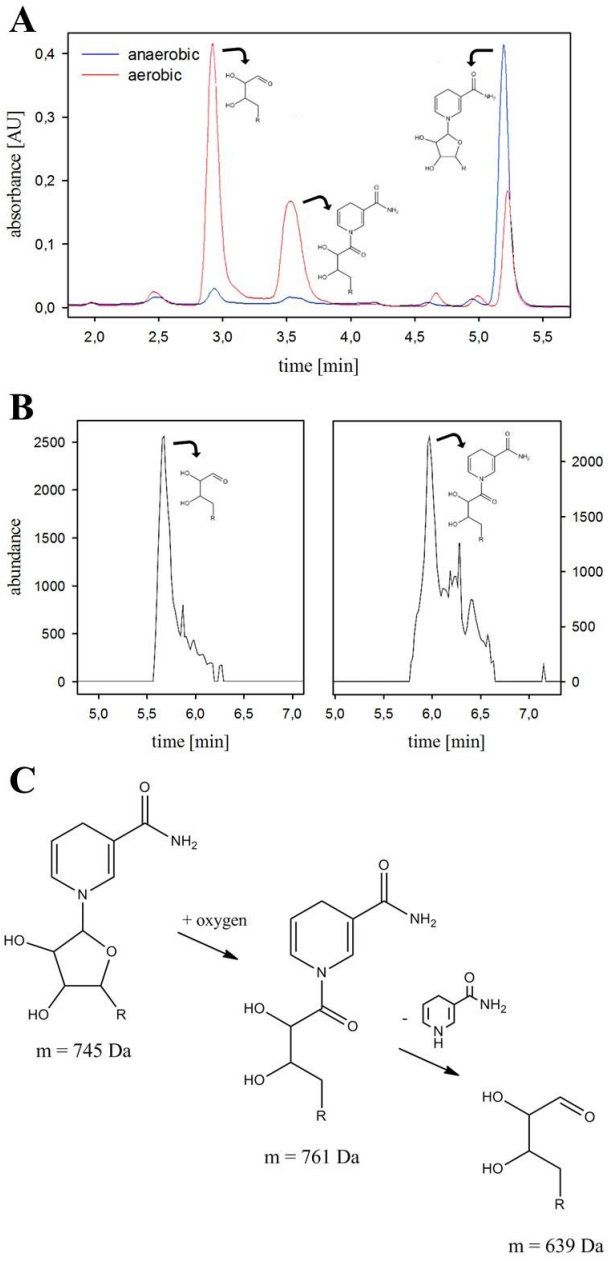

Figure 5: NADPH degradation of the nitrile reductase QueF active site mutant D197A. ***A****: HPLC analysis of degradation products, two products were separated and quantified via HPLC. Blue line: anaerobic conditions, red line: aerobic conditions.* ***B:*** *HPLC-MS analysis of degradation products, two products (m = 639 Da, left graph; m = 761 Da, right graph) were identified via MS.* ***C****: Proposed, oxygen dependent degradation mechanism for NADPH. R = phosphorylated ADP.*

Appendix

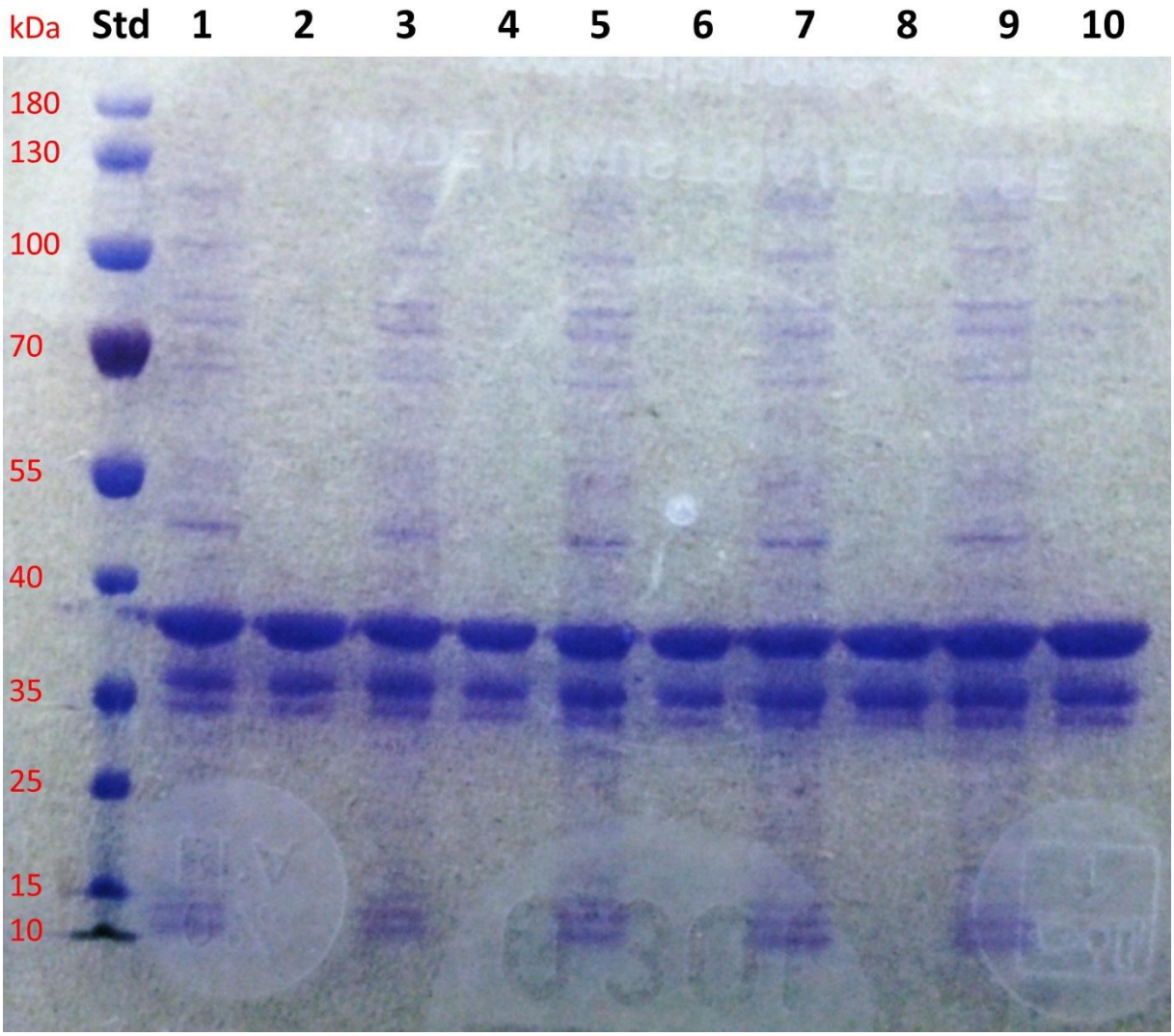

Figure 6: SDS-PAGE gel with cell free extracts from QueF preparations before and after purification with HisTrap protein purification columns. ***Std****: PageRuler™ Prestained Protein Ladder (band sizes given in kDa),* ***1****: wild type before purification,* ***2****: wild type after purification,* ***3****: C190A before purification,* ***4****: C190A after purification,* ***5****: C190S before purification,* ***6****: C190S after purification,* ***7****: D197A before purification,* ***8****: D197A after purification,* ***9****: D197H before purification,* ***10****: D197H after purification. The two bands remaining in the purified fractions represent QueF with and without His-Tag*

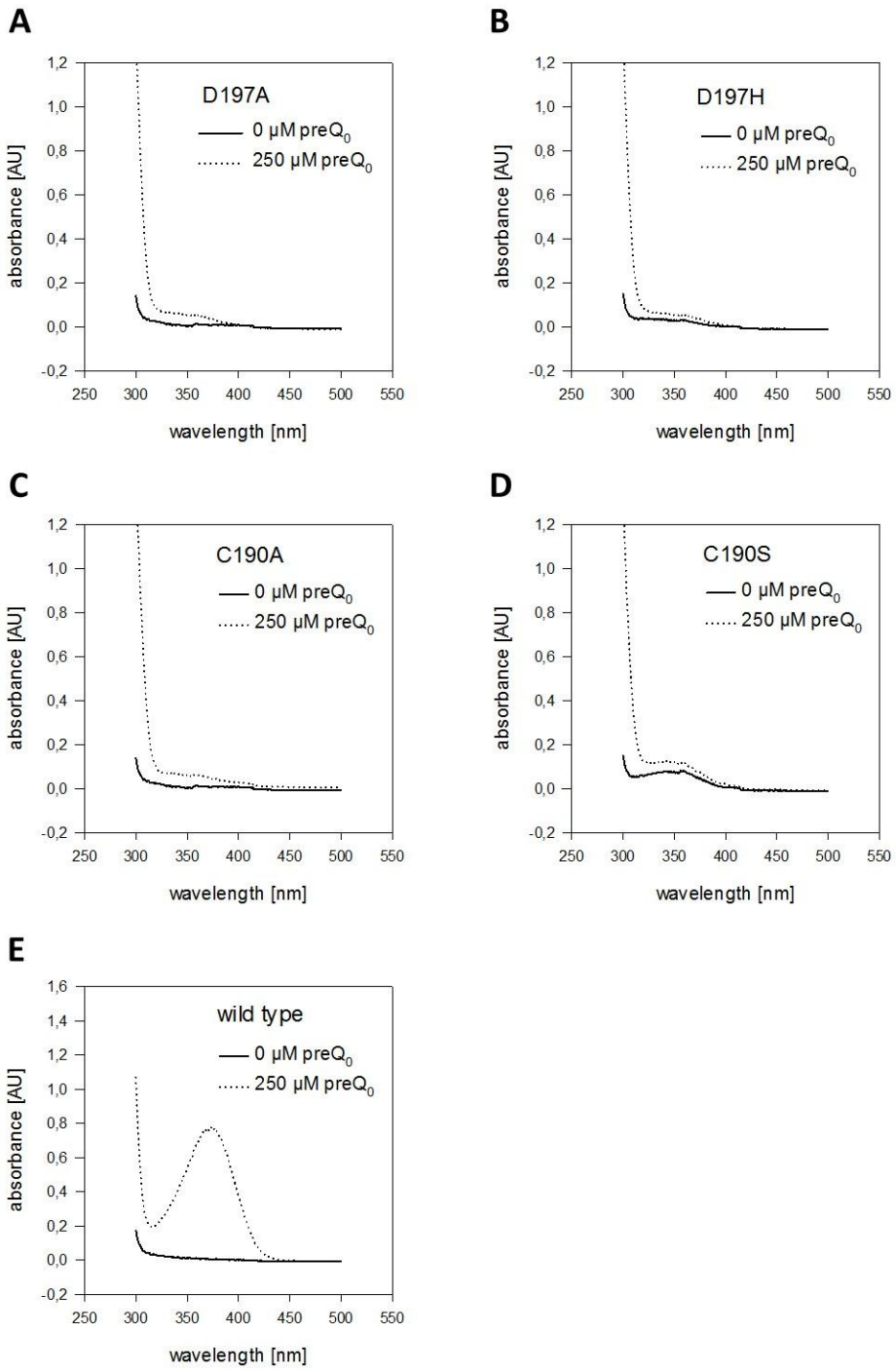

Figure 7: Results of the spectroscopic analysis of covalent enzyme-substrate intermediate formation of QueF mutants and wild type. Solid lines represent samples without substrate, dashed lines represent samples with 250 µM substrate. 50 µM enzyme in all samples. Absorbance maximum at 376 nm indicates covalent adduct. Formation of covalent adduct could not be confirmed for any mutant. ***A****: D197A,* ***B****: D197H,* ***C****: C190A,* ***D****: C190S,* ***E****: wild type*

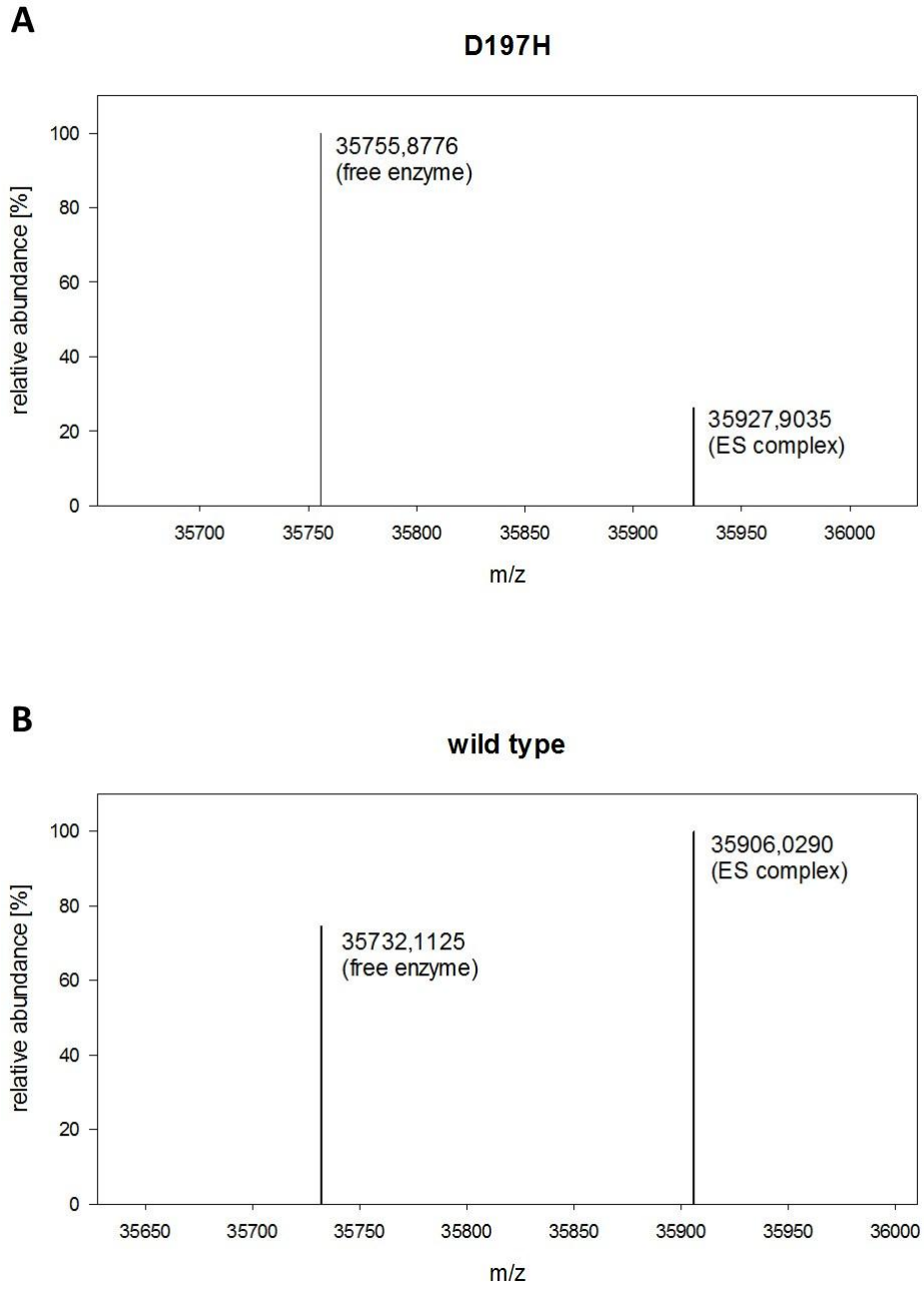

Figure 8: Results of protein-MS analysis of enzyme-substrate complex formation of QueF D197H and wild type. 130 µM enzyme was mixed with 500 µM substrate and analyzed. "Free enzyme" indicates masses correlating to uncomplexed enzyme, "ES complex" indicates masses correlating to the enzyme-substrate complex. Formation of a stable enzyme-substrate complex was confirmed for wild type and D197H. ***A****: D197H,* ***B****: wild type*

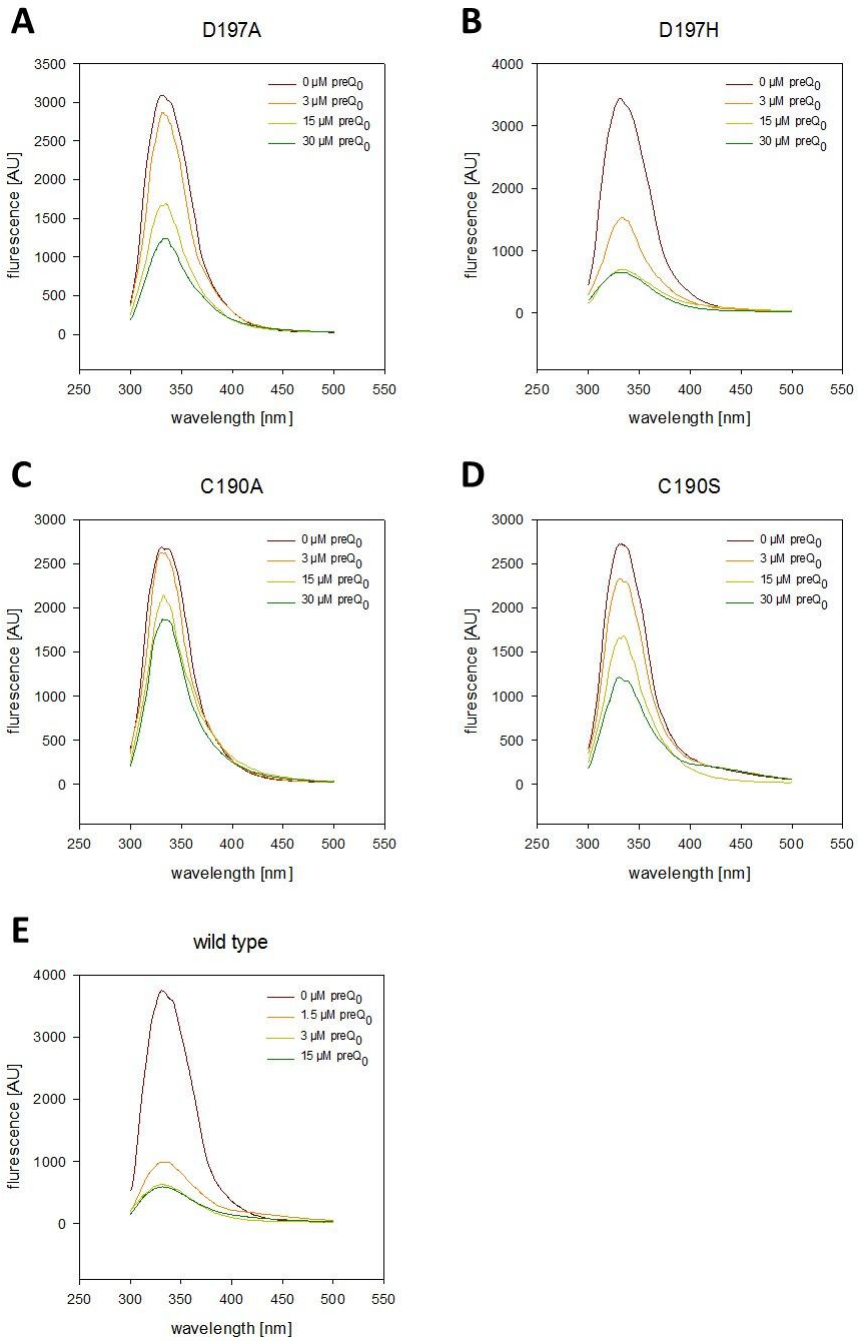

Figure 9: Results of fluorescence quenching analysis of QueF mutants and wild type. 2.8 µM enzyme was mixed with 0, 1.5, 3, 15 or 30 µM substrate and fluorescence was measured. Different colored lines represent increasing substrate concentration. ***A****: D197A,* ***B****: D197H,* ***C****: C190A,* ***D****: C190S,* ***E****: wild type*

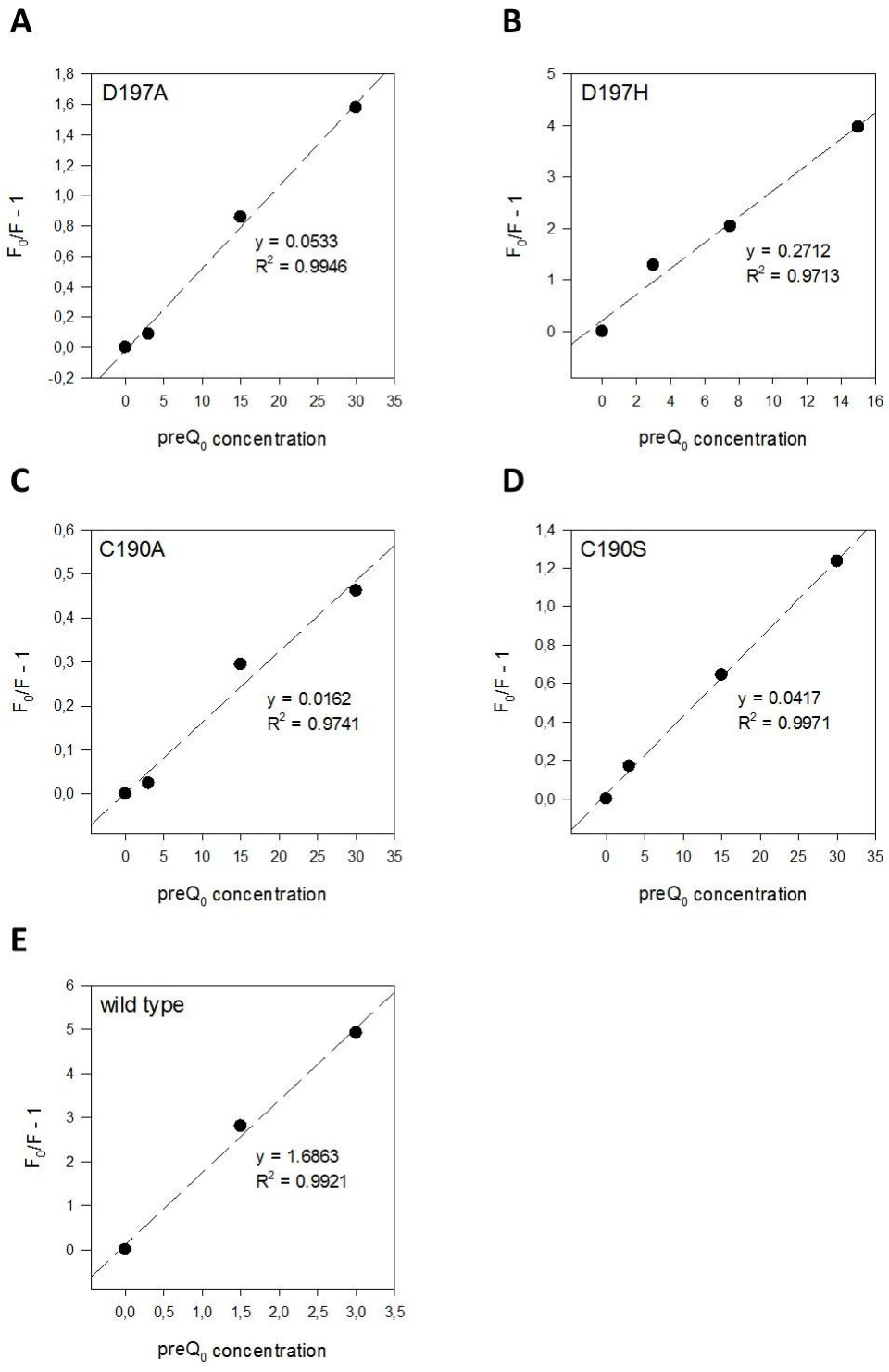

*Figure 10: Results of the Stern-Volmer analysis of QueF mutants and wild type. 2.8 µM enzyme was mixed with 0, 1.5, 3, 7.5, 15 or 30 µM substrate, fluorescence was measured and plotted according to the Stern-Volmer equation. The slope of the resulting line equals the Stern-Volmer constant (K_{SV}). **A**: D197A, **B**: D197H, **C**: C190A, **D**: C190S, **E**: wild type*

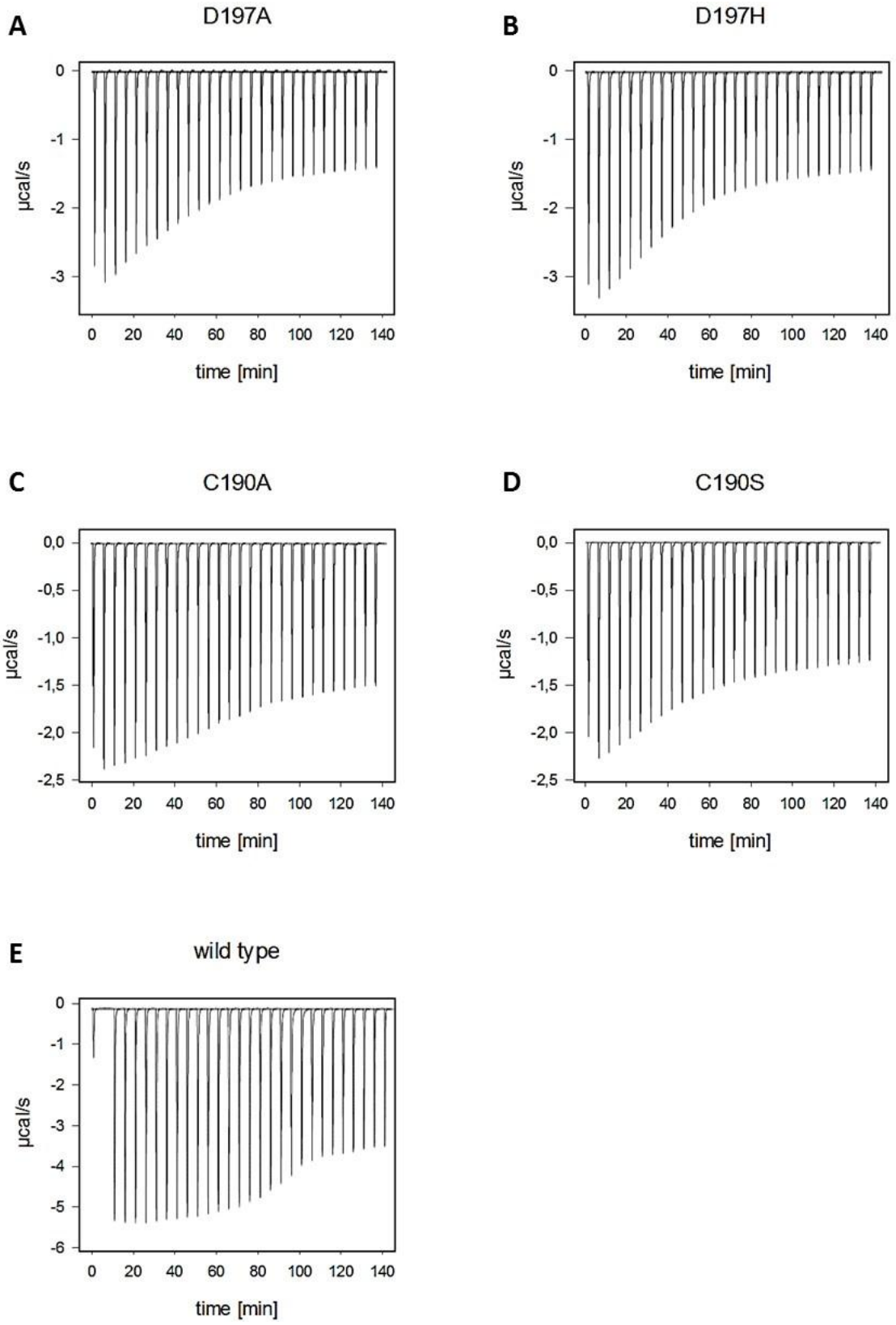

Figure 11: Raw data of the ITC analysis of QueF wild type and mutants. Each peak represents the energy measured for a single injection of 6 µl $preQ_0$ solution (800 µM) into enzyme solution (45 µM). ***A****: D197A,* ***B****: D197H,* ***C****: C190A,* ***D****: C190S,* ***E****: wild type*

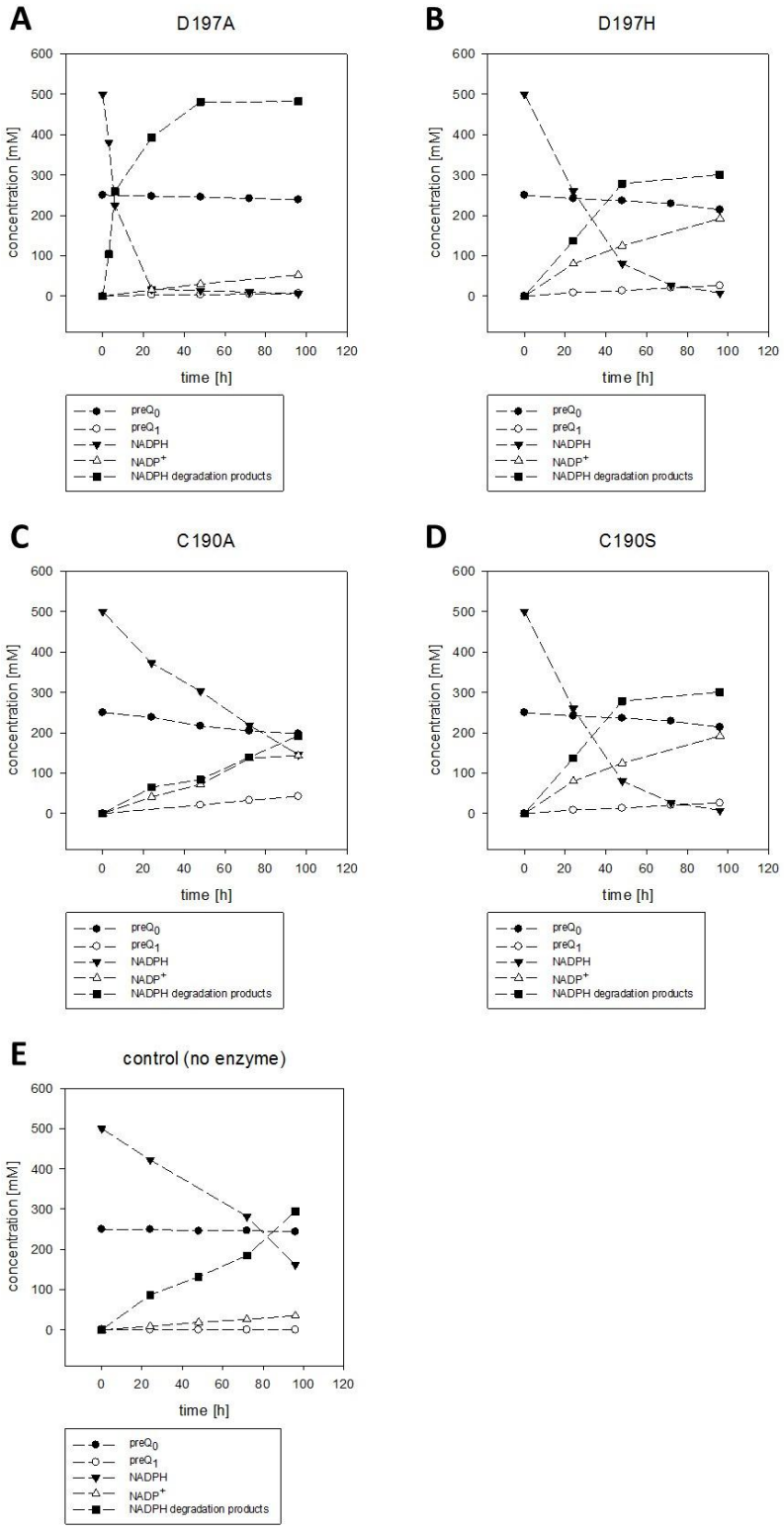

Figure 12: Courses of reactions for QueF mutants, sorted by enzyme variant. 50 µM enzyme (no enzyme in control) was mixed with 250 µM $preQ_0$ and 500 µM NADPH, samples were taken after 0, 3, 6, 24, 48, 72, 96 h and analyzed with HPLC. ***A****: D197A,* ***B****: D197H,* ***C****: C190A,* ***D****: C190S,* ***E****: control*

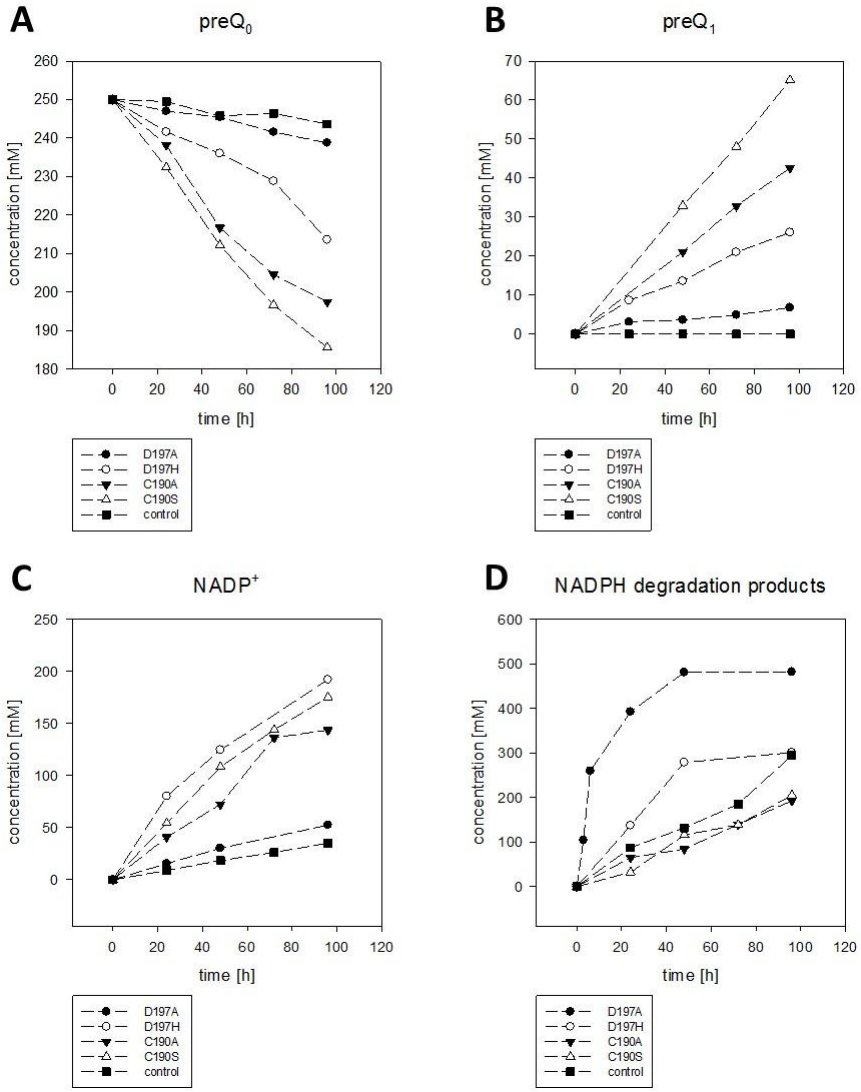

Figure 13: Courses of reactions for QueF mutants, sorted by measured compounds. 50 µM enzyme (no enzyme in control) was mixed with 250 µM $preQ_0$ and 500 µM NADPH, samples were taken after 0, 3, 6, 24, 48, 72, 96 h and analyzed with HPLC. ***A****: $preQ_0$,* ***B****: $preQ_1$,* ***C****: $NADP^+$,* ***D****: NADPH degradation products*

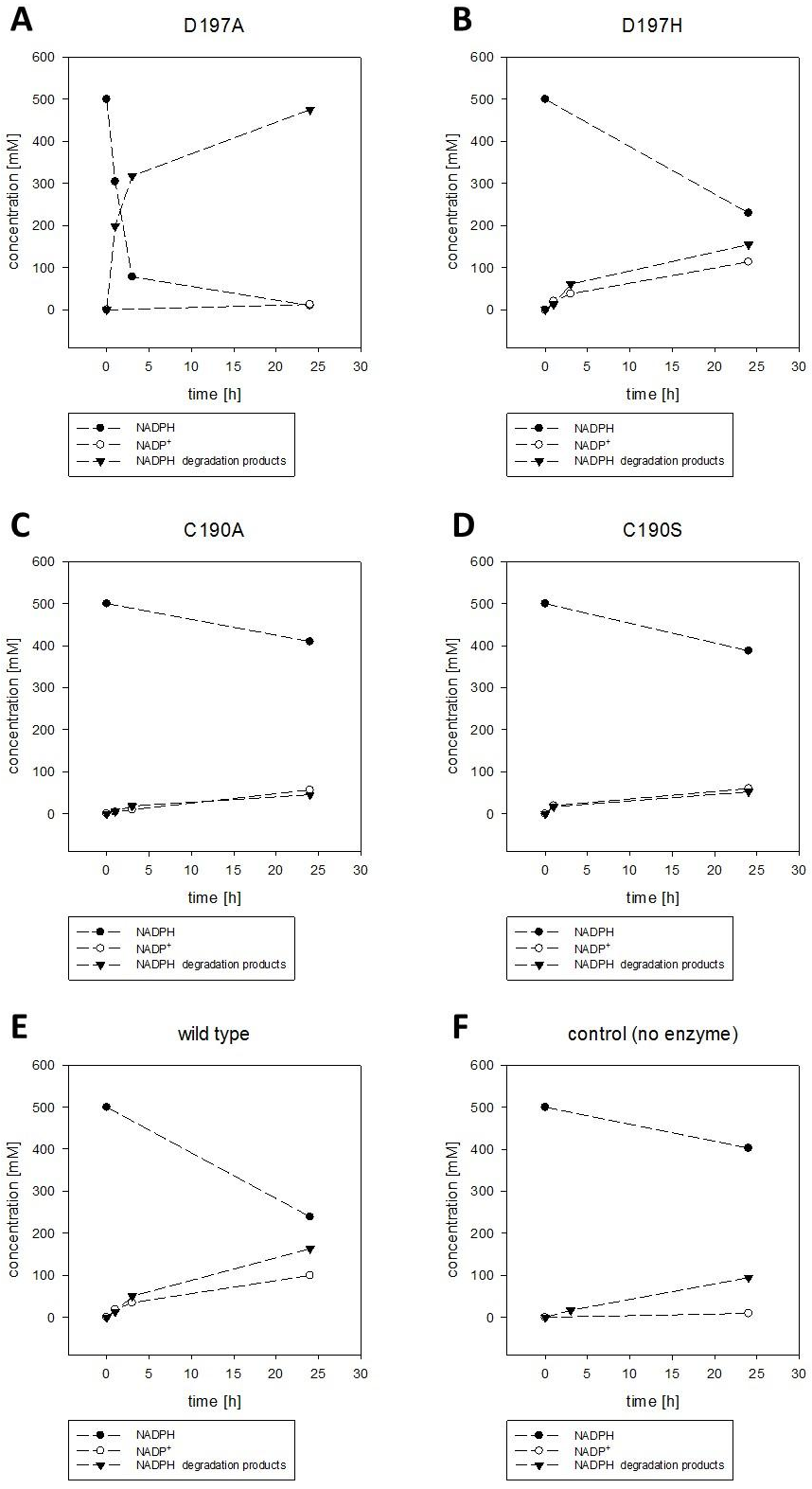

Figure 14: Courses of reactions for QueF mutants and wild type, sorted by enzyme variant. 50 µM enzyme (no enzyme in control) was mixed with 500 µM NADPH, samples were taken after 0, 1, 3, and 24 h and analyzed with HPLC. ***A****: D197A,* ***B****: D197H,* ***C****: C190A,* ***D****: C190S,* ***E****: wild type,* ***F****: control*

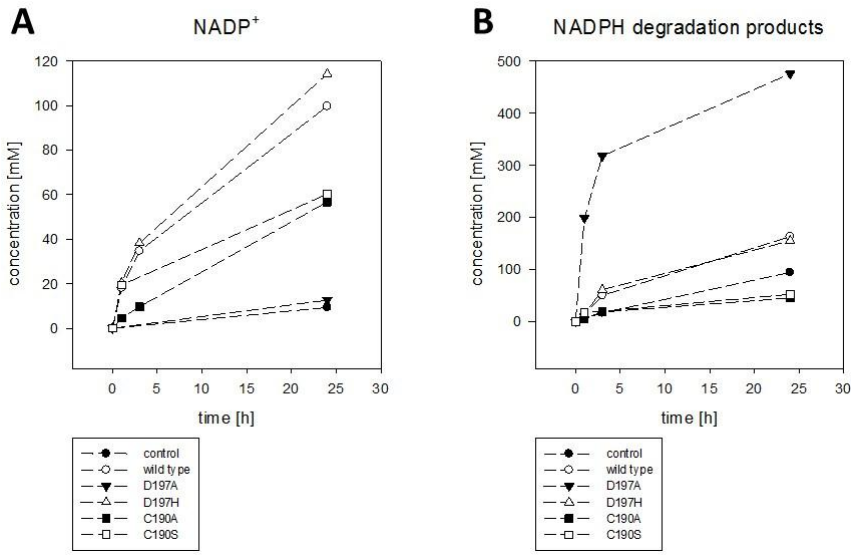

Figure 15: Courses of reactions for QueF mutants and wild type, sorted by measured compounds. 50 µM enzyme (no enzyme in control) was mixed with 500 µM NADPH, samples were taken after 0, 1, 3, and 24 h and analyzed with HPLC. ***A****: NADP*$^+$*,* ***B****: NADPH degradation products*

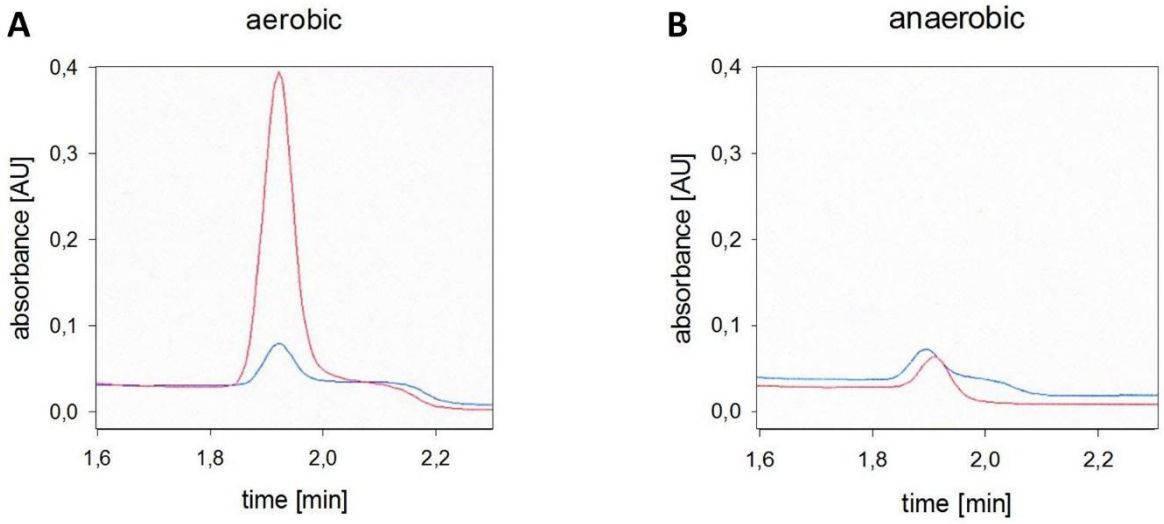

Figure 16: Results of HPLC analysis of NADP$^+$ *production by QueF mutant D197H. 50 µM enzyme (no enzyme in control) was mixed with 500 µM NADPH, samples were taken after 24 h and NADP*$^+$ *concentration was measured. Oxygen dependency of NADP*$^+$ *formation was confirmed.* ***A****: aerobic conditions,* ***B****: anaerobic conditions,* ***blue line****: without enzyme (control),* ***red line****: with enzyme.*

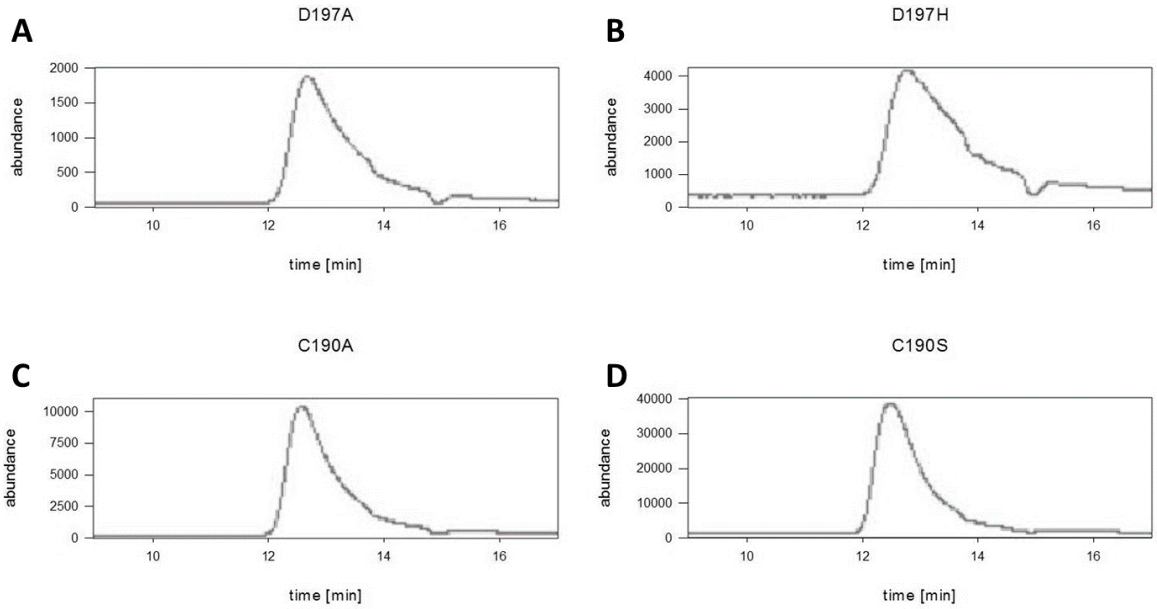

Figure 17: Results of HPLC-MS analysis of QueF mutant $preQ_1$ formation. 50 µM enzyme was mixed with 250 µM $preQ_0$ and 500 µM NADPH, samples were taken after 72 h and analyzed with HPCL-MS. Formation of $preQ_1$ was confirmed for all mutants. ***A****: D197A,* ***B****: D197H,* ***C****: C190A,* ***D****: 190S*